

# Analysis of a digital phase retrieval method for wave-front reconstruction

Wei Huang (黄伟)\*, Dean Liu (刘德安), Xuejie Zhang (张雪洁), Yan Zhang (张燕),  
and Jianqiang Zhu (朱健强)

Shanghai Institute of Optics and Fine Mechanics, Chinese Academy of Sciences, Shanghai 201800, China

\*Corresponding author: august31@mail.usc.edu.cn

Received December 16, 2010; accepted March 15, 2011; posted online June 3, 2011

A phase retrieval algorithm which only needs to measure the intensity distribution at two positions to be effective is used to reconstruct the laser wave-front. Results are obtained from the phase retrieval algorithm in the visible band and the effects of the measurement error on the phase retrieval process are simulated. The algorithm is not sensitive to absolute amplitude measurement error, but is sensitive to the relative distribution of light intensity.

OCIS codes: 010.7350, 100.5070, 260.1960.

doi: 10.3788/COL201109.080101.

Wave-front aberrations that exist in high-power lasers are significant considerations in practical applications because of the dynamic thermal effect and error of appearance surfaces of optical elements. Therefore, it is necessary to develop different kinds of wave-front measurement techniques for the analysis, control, and repair of the wave-front of high-power lasers and for the enhancement of the efficiency of high-power laser systems. In detecting the wave-front distribution, the large variation of phase, high-precision requirements, and compact configuration of systems require a combination of measurement techniques.

Numerous methods have been proposed for the laser wave-front measurement, such as the Shack-Hartmann wave-front sensor and lateral shearing interferometer<sup>[1]</sup>. Despite the simplicity of the Shack-Hartmann sensor, its component, the high-precision lens array, is expensive and difficult to fabricate. Interferometers have high requirements for coherence length and environmental stability and require a complex optical system and image processing algorithms. Fienup *et al.* proposed an algorithm based on Fresnel diffraction for wave-front restoration<sup>[2,3]</sup>. By measuring intensity distributions at two positions in the laser beam propagation and applying the digital algorithm, wave-front phase distributions of the two positions can be calculated. This method is simple, accurate, and free from outside influence. It has been used in the image processing of information optics and astronomy as well. Recently, scholars adopted a similar approach<sup>[4,5,6]</sup> and applied it to the wave-front reconstruction in high-power laser<sup>[7,8]</sup>. For the inevitable measurement error due to experimental conditions in light intensity measurement, the intensity distribution measured by charge-coupled device (CCD) creates a deviation relative to the true intensity distribution, which actually affects the retrieved phase by the algorithm. Currently, no one has yet considered the effects of measurement error on the phase retrieval process. Thus, in this letter, we mainly analyze the influence of changes in the light intensity distribution on the retrieved phase.

The phase retrieval algorithm used in this let-

ter is based on the Fresnel Diffraction formula and the Gerchberg-Saxton and the fienup phase-retrieval algorithms<sup>[9]</sup>. The algorithm has been demonstrated by Matsuoka *et al.*<sup>[8]</sup>.

In Fig. 1, the laser propagates along the  $z$  axis, and the light intensity distributions measured at two planes,  $z = Z_1$  and  $z = Z_2$ , are  $I_1(\xi, \eta)$  and  $I_2(x, y)$ , respectively. The distance between the two planes is  $Z = Z_2 - Z_1$ . The corresponding amplitudes are obtained using

$$u_1(\xi, \eta) = \sqrt{I_1(\xi, \eta)}, \quad (1)$$

$$u_2(x, y) = \sqrt{I_2(x, y)}. \quad (2)$$

According to the Huygens-Fresnel principle, under the condition of Fresnel approximation, the relationship between the wave functions at the two planes is<sup>[10]</sup>

$$U_2(x, y) = \frac{e^{ikZ}}{i\lambda Z} e^{i\frac{k}{2Z}(x^2+y^2)} \iint_{-\infty}^{\infty} [U_1(\xi, \eta) e^{i\frac{k}{2Z}(\xi^2+\eta^2)} \cdot e^{-i\frac{2\pi}{\lambda Z}(x\xi+y\eta)} d\xi d\eta. \quad (3)$$

In the diffraction integral formula,

$$U_1(\xi, \eta) = u_1(\xi, \eta) \exp[i2\pi\varphi_1(\xi, \eta)], \quad (4)$$

$$U_2(x, y) = u_2(x, y) \exp[i2\pi\varphi_2(x, y)], \quad (5)$$

where  $\varphi_1$  and  $\varphi_2$  are phase distributions at planes  $z = Z_1$  and  $z = Z_2$ , respectively.

Figure 2 shows the flowchart of the algorithm. To

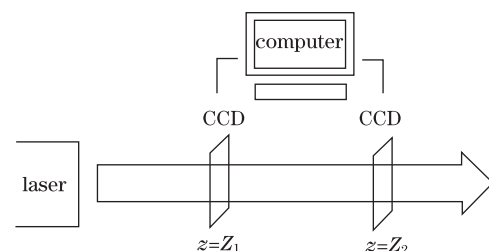


Fig. 1. Experimental schematic diagram.

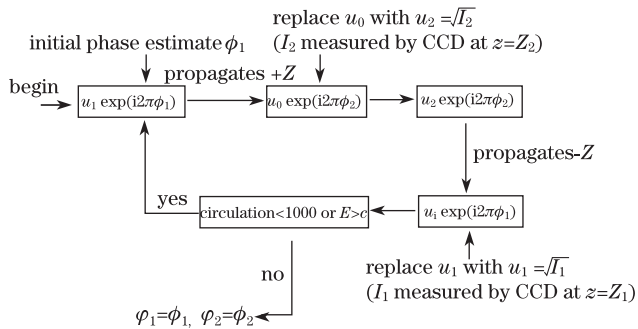


Fig. 2. Flowchart of the algorithm.

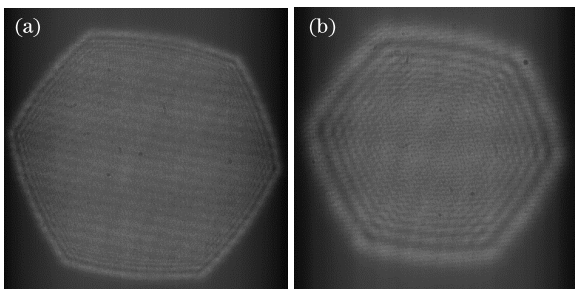


Fig. 3. Intensity distribution measured by CCD. (a)  $z=Z_1$ ; (b)  $z=Z_2$ .

obtain the phase distributions at the two planes, the algorithm follows the steps described in Fig. 2. When the algorithm stops, the phase distributions  $\varphi_1$  and  $\varphi_2$  at the two planes are retrieved as  $\varphi_1 = \phi_1$  and  $\varphi_2 = \phi_2$ . As a result, the reconstruction of the wave-front is realized.

Using the He-Ne laser ( $\lambda=632.8$  nm) in Zygo interferometer ( $\phi=60$  mm) as the light source, the obtained distance between  $z = Z_1$  and  $z = Z_2$  is 0.25 m. We observed the first direct optical alignment, and subsequently recorded the intensity distributions at the two planes using a CCD camera. Figures 3(a) and (b) are the intensity distributions at planes  $z = Z_1$  and  $z = Z_2$ , respectively.

Substituting the experimental data into the algorithm and setting the iteration time at 1,000, we obtain the phase distributions at the two planes  $z = Z_1$  and  $z = Z_2$ , as shown in Fig. 4. The wave-front reconstructed at  $z = Z_1$  is  $0.6509\lambda$  peak-valley (PV) and  $0.0626\lambda$  root mean square (RMS) resulted in  $0.4806\lambda$  PV and  $0.0672\lambda$  RMS at  $z = Z_2$ , after correction.

To determine the proximity between the measurement result and calculated result, we defined parameter  $E$  as

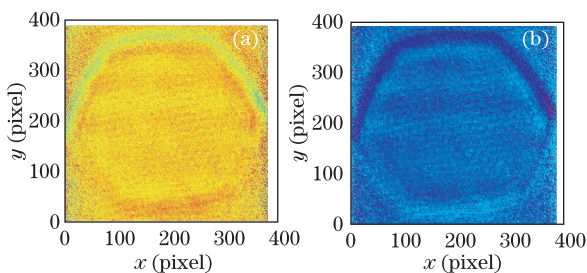


Fig. 4. Phase distribution calculated by the algorithm. (a)  $z=Z_1$ ; (b)  $z=Z_2$ .

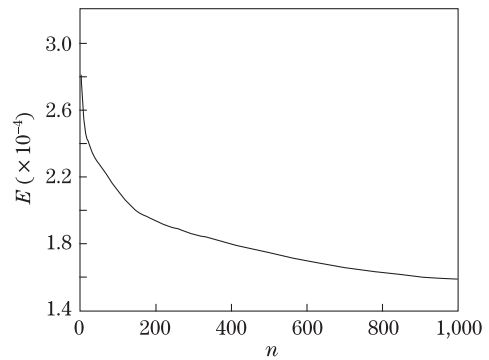


Fig. 5. Relationship of  $E$  and iteration times  $n$ .

$$E = \frac{\sqrt{\sum [I_1(\xi, \eta) - I_i(\xi, \eta)]^2}}{\sum I_1(\xi, \eta)}, \quad (6)$$

where  $I_1$  is the measured intensity distribution at  $z = Z_1$  and  $I_i$  is the calculated intensity ( $I_i = u_i^2$ ). Figure 5 shows the relationship between  $E$  and iteration times  $n$ . The value of  $E$  decreases with the increase of iteration times, which indicates that the difference between the measurement result and calculated result will be smaller when the iteration times are increased.

In the actual measurements, the measured intensity distribution deviation will exist because of the presence of measurement error. This is not the case with the true intensity distribution. The fluctuation of the light source would affect the absolute amplitude measurement result. The interference from the background light and the shaken environment would generate an uncertain random

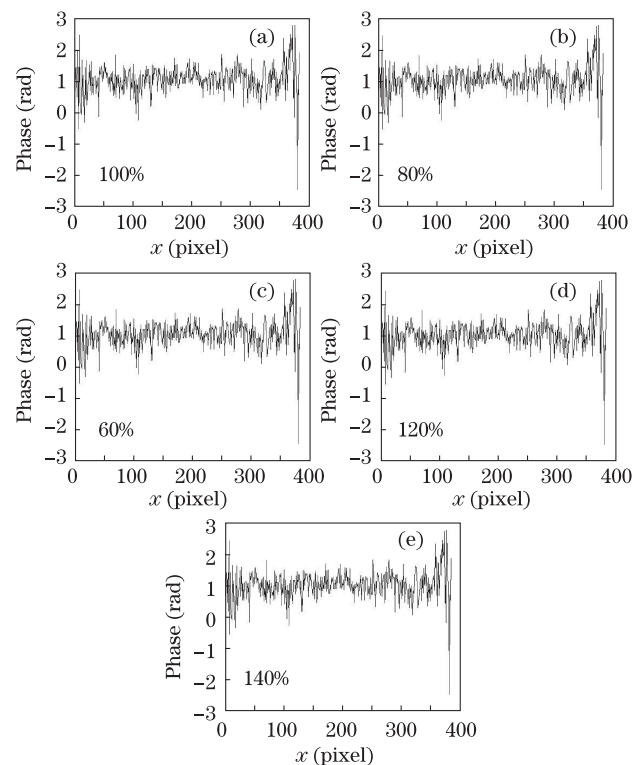


Fig. 6. (Color online) 1D distribution of the retrieved phase when the proportion of intensity distribution at the two measuring faces changed.

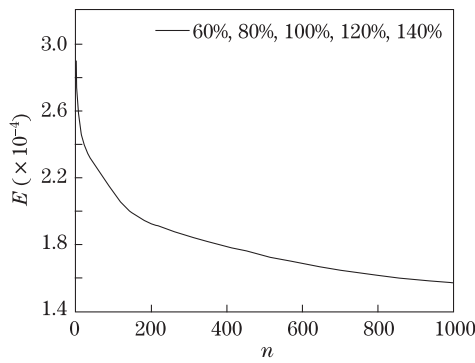


Fig. 7. Relationship of  $E$  and iteration times  $n$  when intensity distribution at both two measuring faces changed in proportion.

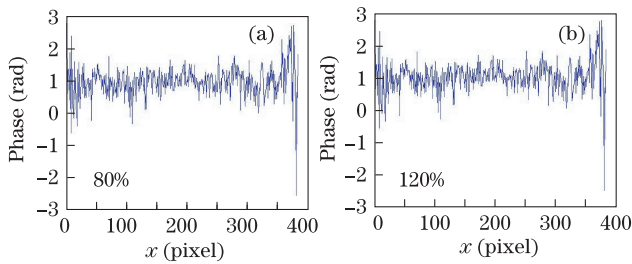


Fig. 8. 1D distribution of the retrieved phase when the intensity distribution at measuring face  $z = Z_1$  changed in proportion.

measurement error, and the airborne dust on the laser beam would lead to local measurement error. Based on these considerations, we simulated three situations: 1) variation of full aperture light intensity; 2) intensity distribution at measuring face with random measurement error; 3) intensity distribution at the measuring face with local measurement error.

The two images measured by CCD in Matlab were processed. Subsequently, we changed the two corresponding matrix values into 60%, 80%, 120%, and 140%, incorporated these data into the algorithm, and recovered the phase distribution. After analyzing the one-dimensional (1D) information of the obtained experimental results and the relationship between  $E$  and iteration times under the different situations above, the curves are completely similar and no difference among the experimental results presented exists, as shown in Figs. 6 and 7. Meanwhile, the retrieved phase remains unchanged.

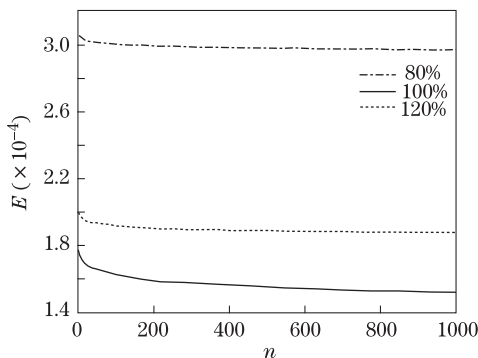


Fig. 9. Relationship of  $E$  and iteration times  $n$  when intensity distribution at measuring face  $z = Z_1$  changed in proportion.

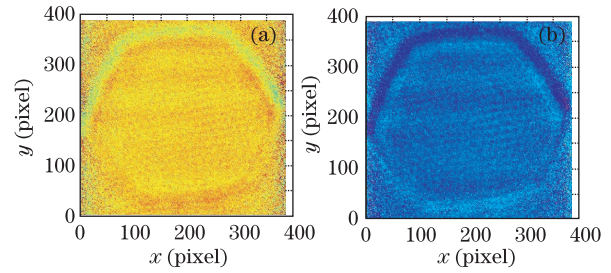


Fig. 10. Phase distribution with random error. (a)  $z = Z_1$ ; (b)  $z = Z_2$ .

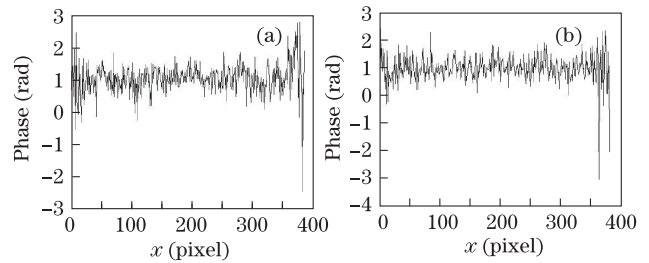


Fig. 11. Analysis of a particular dimension of the two recovery phases. Simulation result (a) without and (b) with random error.

We only changed one original matrix value (the matrix corresponding to image measured in plane  $z = Z_1$  is chosen) into 80% and 120%. In both cases, the retrieved phase distributions are the same as those obtained when the matrix value is not changed, as shown in Fig. 8. At the same time, Fig. 9 indicates that under the two situations, the values of  $E$  are both larger than its value when the matrix is unchanged. However, the values continue to decrease with the increase of iteration times. Based on these, we conclude that the results of the phase retrieval are not affected by the absolute value of the intensity. Instead, the results are affected by the relative distribution of intensity.

We used Matlab to read the CCD images and added a random error to one of the intensity distributions (maximum intensity 115). The error matrix ranges from  $-7$  to  $7$ , which was produced by a random number generator. By changing the intensity distribution, a new phase of distribution was obtained. The simulation result is shown in Fig. 10. Figures 10(a) and (b) show the phase distributions at  $z = Z_1$  and  $z = Z_2$ , respectively. The wave-front reconstruction of the central part at  $z = Z_1$

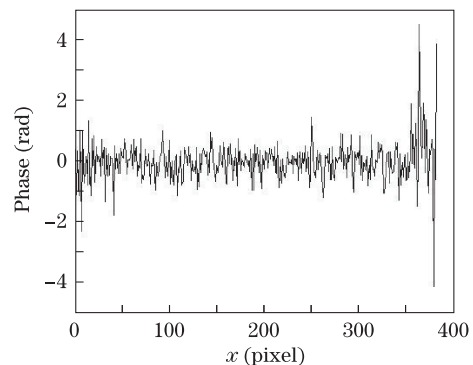


Fig. 12. Difference between the two retrieved phases.

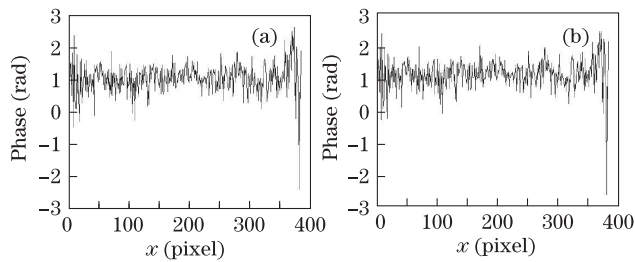


Fig. 13. 1D distribution of the retrieved phase with local measurement error at one measuring face  $z = Z_1$ . 1D distribution of the retrieved phase with error matrix consisting of elements that are all (a) 7 and (b) 20.

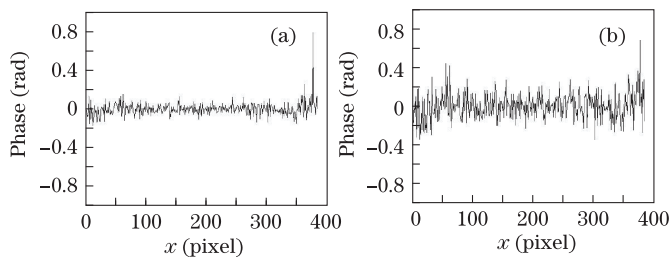


Fig. 14. Difference of the retrieved phases when a local measurement error exists with the retrieved phase; measured data remain unchanged. Error matrix consisting of elements that are all (a) 7 and (b) 20.

is  $0.6135\lambda$  PV and  $0.0635\lambda$  RMS. Values obtained after correction are  $0.4650\lambda$  PV and  $0.0687\lambda$  RMS at  $z = Z_2$ .

Post-analysis of a particular dimension of the retrieved phase and the comparison with the dimension obtained prior to the addition of random errors are shown in Fig. 11. A high degree of similarity between the dimensions can be observed. Figure 11(a) is the simulation result of a particular dimension distribution of the recovery phase without random error. Figure 11(b) is the simulation result with random error. The difference between the two retrieved phases is shown in Fig. 12. Based on the analysis of the difference between the two retrieved phases, the resulting average difference is  $0.0688\lambda$  and the RMS is  $0.1024\lambda$ . Therefore, this algorithm has high tolerance.

To simulate the influence of the local measurement error on the retrieved phase, a  $6 \times 6$  matrix containing elements that are all 7 was added to the point ( $x=y=128$  pixel) of the matrix corresponding to the image measured at plane  $z = Z_1$ . Using the phase retrieval method shown above, a new phase distribution was obtained. The particular dimension is shown in Fig. 13(a). Similarly, we obtained the phase distribution with local measurement error of a  $6 \times 6$  matrix containing elements that are all 20. Consequently, the phase information of the same dimension was extracted, which is shown in Fig. 13(b). Meanwhile, Fig. 14 shows the difference between the

retrieved phase without measurement error and the one with local measurement error. Figures 14(a) and (b) correspond to the error matrix containing elements that are all 7 and 20, respectively. Against the dimension, with an error matrix consisting of elements that are all 7, the average difference is  $0.0070\lambda$  and the RMS is  $0.0123\lambda$ . In the error matrix with elements that are all 20, the average difference is  $0.0167\lambda$  and the RMS is  $0.0565\lambda$ . Therefore, we conclude that local measurement error can affect the overall phase retrieval results. However, the influence is weak against the high tolerance of the algorithm.

In conclusion, we describe a phase retrieval algorithm based on the Fresnel diffraction formula and the Gerchberg–Saxton and the fienup phase-retrieval algorithms. The feasibility of this numerical algorithm is demonstrated. Considering that the intensity of the image captured by CCD is different from its real intensity in the actual measurement, we simulate that the full aperture intensity distribution changes in proportion and the intensity distribution with random measurement error. If amplitude variation of full aperture light intensity changes proportionally, then the result of the phase retrieval does not change because it is affected not by the absolute value of the intensity, but by the relative distribution of the intensity. If the intensity distribution with random error occurs, the result of the phase retrieval is very similar to the result in the absence of error. If the local measurement error in intensity distribution is produced, the retrieved phase is affected not only in the local location, but in the whole distribution as well. However, the effect is weak. Based on the analysis of the above-mentioned types of light intensity change, it can be inferred that this algorithm has high tolerance.

## References

1. D. Malacara, *Optical Shop Testing* (2nd edn.) (Wiley-Interscience, New York, 1992).
2. J. R. Fienup, *Appl. Opt.* **32**, 1737 (1993).
3. G. R. Brady and J. R. Fienup, in *Proceedings of in Frontiers in Optics, OSA Technical Digest OFWAS* (2006)
4. G. Yang, B. Dong, B. Gu, J. Zhuang, and O. K. Ersoy, *Appl. Opt.* **33**, 209 (1994).
5. P. Yang, M. Ao, B. Xu, and X. Yuan, *Appl. Opt.* **48**, 1402 (2009).
6. Z. Ma, H. Li, and X. Lü, *Chin. Opt. Lett.* **7**, 1076 (2009).
7. S. W. Bahk, J. Bromage, and J. D. Zuegel, in *Proceedings of CLEO/QELS JThBb* (2008).
8. S. Matsuoka and K. Yamakawa, *J. Opt. Soc. Am. B* **17**, 663 (2000).
9. J. R. Fienup, *Appl. Opt.* **21**, 2758 (1982).
10. J. W. Goodman, *Introduction to Fourier Optics* (3rd edn.) (Los Altos, California, 2006).